

SYNTHESIS AND CHARACTERIZATION OF H-BORON NITRIDE BY UREA ROUTES

Majid Amishi, Farhad Moravvej-Farshi, Saied Abbasalizadeh, Khanali nekouee*

Faculty of Materials and Manufacturing Technologies, Malek Ashtar University of Technology, Tehran, Iran

INTRODUCTION

Boron nitride in all its various structures is a man-made product and is not found in nature. Boron and nitrogen are carbon neighbours in the periodic table, so boron nitride phases are equivalent to carbon-related phases[1,2]. The first synthesis for boron nitride was proposed in 1842 by Balmain, using molten boric acid and potassium cyanide as raw materials, but the resulting composition was unstable. Efforts continued until in 1957, Ventorf successfully synthesized high temperature, high pressure, and cubic boron nitride in a similar way to diamond synthesis [3,4].

Hexagonal boron nitride is commonly called (h-BN), but is also referred to as (α -BN) or (g-BN (graphitic-BN)[4,5]. Special properties of boron nitride are: high thermal conductivity ($30-100 \text{ w.m}^{-1}\text{.k}^{-1}$) [6], low thermal expansion ($0.5-12 \times 10^{-6} /^\circ\text{C}$) [7], good thermal shock resistance [8], high electrical resistance ($>10 \Omega$) [9], low dielectric constant [10], low density (2.27 g/cm^3) [11], microwave transparency, non-toxic easy machining, non-abrasive and lubricating, chemical stability [12,13]. Special features of boron nitride include its dielectric properties (with a dielectric constant of 4 at frequencies in the GHz range, i.e. half the dielectric constant of $\alpha\text{-Al}_2\text{O}_3$ [14]), as well as its high dielectric strength and lubricating ability in the wide range of temperature. The low friction coefficient of this material is maintained up to 900°C , while other solid lubricants such as graphite and molybdenum disulphide burn at low temperatures [15]. Because of the high temperature stability of boron nitride and its resistance to carbon and carbon monoxide up to 1800°C , it acts as a better refractory ceramic material than nitride ceramics such as Si_3N_4 [1,16,17].

MATERIALS AND METHODE

Materials

For the synthesis of hexagonal boron nitride powder, boric acid and urea were used as raw materials. Acid leaching of samples was also performed with nitric acid. All materials with high purity were provided by the Merck Company, Germany and used as received without any purification.

Synthesis procedure

First, boric acid and urea were weighed to prepare samples with molar ratios of boric acid to urea 1:5 and 1:7, respectively, and dissolved separately in deionized water at 80°C . After adding two solutions to each other, a wet milling was used for 5 hours in order to provide mechanochemical energy for the reaction of raw materials with each other [18]. The resulting mixture was dried at 120°C for 2 hours. The powder obtained in this step was placed in a quartz tube furnace with a temperature of 1200°C and different times of 3 and 5 hours in order to provide the thermodynamic conditions of the reaction.

In order to supply the necessary nitrogen for the reaction, a nitrogen gas atmosphere was used in the furnace. The samples obtained from each step were named according to Table 1. After this step, to remove carbonaceous impurities, the samples were heat-treated for 2 hours at 850°C in an oxidizing atmosphere.

Table 1: The order of naming the samples.

Sample name	Molar ratio	Reaction time (hours)
$\text{C}_{1.5}\text{T}_3$	1:5	3
$\text{C}_{1.7}\text{T}_3$	1:7	3
$\text{C}_{1.5}\text{T}_5$	1:5	5
$\text{C}_{1.7}\text{T}_5$	1:7	5



Figure 1: Final shape of sample $\text{C}_{1.5}\text{T}_5$.

Finally, acid leaching was used to remove the remaining boric acid and other impurities. A mixture of water and nitric acid (with 1:1 ratio) was prepared. The powders were dissolved in it for 1 hour and passed through a paper filter. The final shape of the $\text{C}_{1.5}\text{T}_5$ sample is shown in Figure 1.

RESULTS AND DISCUSSION

Structural characterization

The XRD patterns from the synthesized samples with different boric acid to urea ratios and different reaction times are shown in Figure 2. The peak in the range $2\theta = 42.5^\circ$ and $2\theta = 26.7^\circ$ corresponds to the most well-known hexagonal boron nitride atomic plates (002) and (100) (JCPDS card no. 34-0421) [21-19]. The diffraction background indicated that an amorphous phase structure was formed for all samples. In samples $\text{C}_{1.5}\text{T}_3$ and $\text{C}_{1.7}\text{T}_3$, which were heat-treated in the furnace for three hours, the peak of impurity was observed at $2\theta = 27.88^\circ$. This peak is related to boron oxide B_2O_3 (JCPDS card no. 06-0297) which is result of excess or non-reacted boric acid. As the heat-treatment time increased to 5 hours and the reaction was complete, this peak was eliminated in the $\text{C}_{1.5}\text{T}_5$ and $\text{C}_{1.7}\text{T}_5$ samples.

Boric acid has been used as a source of boron and urea has been used as a source of nitrogen and reducing agent. According to the obtained results, it is observed that with increasing the molar ratio of urea, the amount of nitrogen introduced into the reaction increases. By comparing the XRD patterns of $\text{C}_{1.5}\text{T}_5$ and $\text{C}_{1.7}\text{T}_5$ (Figure 2), it can be concluded that by increasing the molar ratio of urea from 5 in sample $\text{C}_{1.5}\text{T}_5$ to 7 in sample $\text{C}_{1.7}\text{T}_5$, the impurity peak formed in the sample with more urea ($\text{C}_{1.7}\text{T}_5$) which is related to carbon dioxide (CO_2). We conclude that by increasing the molar ratio of urea to a certain limit, the excess amount of this substance will not be consumed in the reaction and will form the impure phase of CO_2 . The crystallite size of the synthesized powders was calculated by Williamson-Hall method and is given in Table 2. The lowest crystallite size was reported with 10.4 nm for sample $\text{C}_{1.5}\text{T}_5$.

Table 1: Crystallite size of different samples.

Sample	$\text{C}_{1.5}\text{T}_3$	$\text{C}_{1.7}\text{T}_3$	$\text{C}_{1.5}\text{T}_5$	$\text{C}_{1.7}\text{T}_5$
2θ	26.61	26.6	26.7	27.13
Crystallite size	25.9	34.6	10.4	14.8

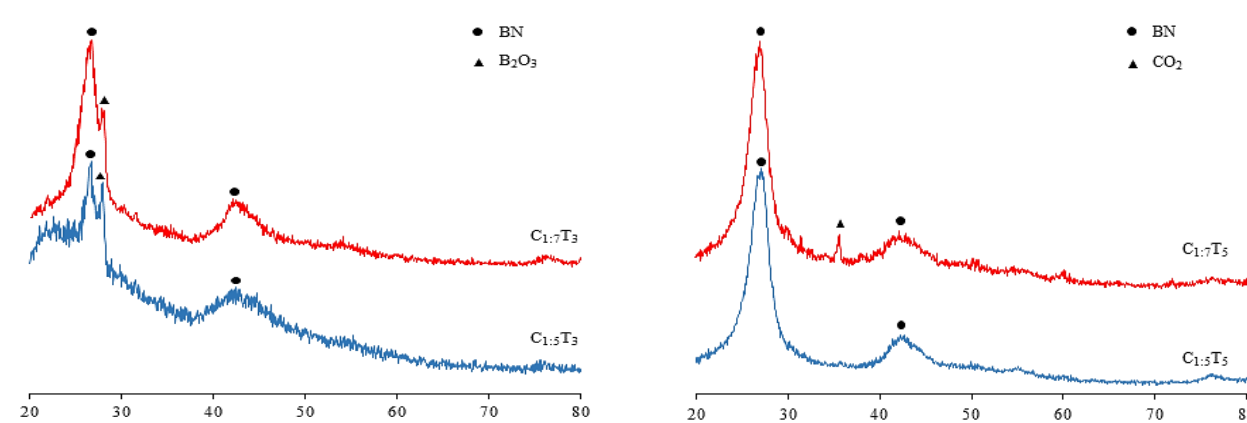


Figure 2: XRD patterns of synthesized samples.

Microstructural Characterization

Figures 3 (a), (b) and (c) show scanning electron microscope (SEM) images of the synthesized powder $\text{C}_{1.5}\text{T}_5$ at different magnifications. Figure 3 (a) shows that the resulting powder has a grain structure with a smooth surface. In Figure 3 (b), the powder is agglomerated and is seen as a layer. This agglomeration can be due to high crystallization and fine particles synthesized without the use of catalysts [22]. In addition, Figure 3 (c) shows the layered structure of the synthesized powder, which indicates complete crystallization and confirms the formation of h-BN nanocrystals.

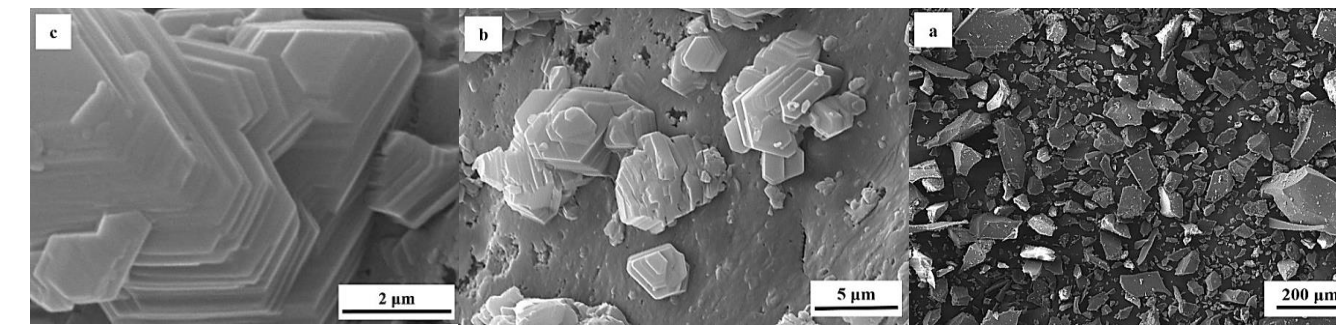


Figure 3: SEM images related to sample $\text{C}_{1.5}\text{T}_5$

Chemical Characterization

In order to evaluate the chemical bonds formed in the samples after the completion of the synthesis steps, Fourier transform infrared spectroscopy (FTIR) and X-ray photoelectron spectroscopy (XPS) were used. The spectrum of the FTIR analyse from sample $\text{C}_{1.5}\text{T}_5$ is shown in Figure 4. The peaks in 3208 and 1413 , 1181 , 715 cm^{-1} belong to the B-N and BN-O bands, which are attributed to hexagonal and B-OH nitride bonds, respectively. The strong absorption peak at 1400 and 780 cm^{-1} is also related to B-N tensile and bending vibration, respectively [19]. Thus the FTIR analyse confirms the formation of hexagonal boron nitride and the results of XRD showed it. The chemical conditions of the synthesized $\text{C}_{1.5}\text{T}_5$ samples were examined using XPS analyse. Figure 5 shows that the surface of sample consist of B and N as main elements and carbon and oxygen as impurities elements. Figure 5 (b), (c), (d) show the spectra B 1s, C 1s and N 1s. The spectrum of B 1s in Figure 5 (b) is characterized by the peak B-N at 193.3 eV . The N 1s spectrum is characterized by a B-N peak at 399.2 eV (Figures 4 (c)).

CONCLUSIONS

- Boric acid reduction by urea routes is one of the most cost-effective methods of boron nitride production that is used to industrial scale.
- The appropriate ratio of boric acid to urea as raw materials was determined to be 1:5, because by increasing the amount of urea from a certain limit, the impure phase of carbon dioxide (CO_2) is formed.
- The reaction was performed for 3 and 5 hours and it was observed that with increasing time, the reaction was more complete, the boron oxide impurity was removed and in total, boron nitride would have a high purity.
- The second stage of heat treatment at 850°C and oxidized atmosphere caused the burning of excess carbon and the removal of impurity phases such as B_2O_3 .
- Acid leaching was determined as one of the important steps in the synthesis of hexagonal nitride boron powder for removal of impurities.
- The results of the XRD test were reported and the peaks in the range $2\theta = 42.5^\circ$ and $2\theta = 26.7^\circ$, which correspond to the most well-known hexagonal boron nitride atomic plates (002) and (100) approved hexagonal boron nitride synthesis.
- The crystallite size of samples was calculated by Williamson-Hall method, which was reported between 10.4 to 61.4 nm . The lowest value is for sample $\text{C}_{1.5}\text{T}_5$.
- The results of the FTIR test were reported and the peaks in the values of 3208 and 1413 , 1181 , 715 cm^{-1} of the B-N bands attributed to the hexagonal nitride bonds confirmed the synthesis of hexagonal boron nitride.
- The results of XPS test were reported and the successful synthesis of hexagonal boron nitride was confirmed based on the peaks of the B-N bond present on the surface of the material.
- Sample $\text{C}_{1.5}\text{T}_5$ was determined as optimal sample, which did not contain any impurities.



Figure 4: FTIR spectrum of sample $\text{C}_{1.5}\text{T}_5$.

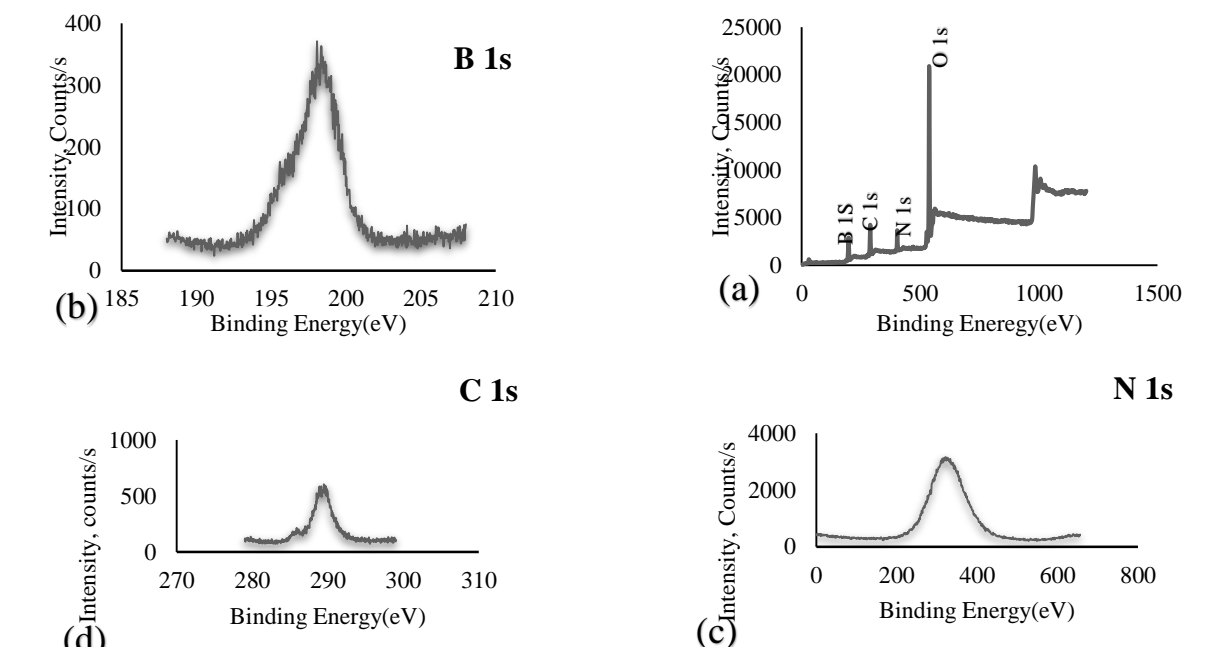


Figure 5: XPS spectra of sample $\text{C}_{1.5}\text{T}_5$.

REFERENCES

- B. Ertuğ, "Powder preparation, properties and industrial applications of hexagonal boron nitride," vol. 33, 2013.
- A. A. Gromov and L. N. Chukhlova, Nitride ceramics: combustion synthesis, properties and applications. John Wiley & Sons, 2015.
- A. Lipp, K. A. Schwetz, and K. Hunold, "Hexagonal boron nitride: fabrication, properties and applications," vol. 5, no. 1, pp. 3-9, 1989.
- F. Aldinger, S. Frühauf, U. Herzog, B. Jäschke, T. Jäschke, E. Müller, G. Roewer, H.J. Seifert, and K. Trommer, High performance non-oxide ceramics I. Springer, 2003.
- B. Matovic B. Babic, A. Devecerski, M. Radovic, A. Minovic, M. Mijlkovic, S. Boskovic, "New synthetic route for nanocrystalline boron nitride powder," vol. 65, no. 2, pp. 307-309, 2011.
- I. Jo, M.T. Pettes, J. Kim, K. Watanabe, T. Taniguchi, Z. Yao, L. Shi, "Thermal conductivity and phonon transport in suspended few-layer hexagonal boron nitride," vol. 13, no. 2, pp. 550-554, 2013.
- X. Hou, Z. Yu, Y. Li, and K. Chou, "Preparation and properties of hexagonal boron nitride fibers used as high temperature membrane filter," vol. 49, pp. 39-43, 2014.
- W. Paszkowicz, J. Pelka, M. Knapp, T. Szyzsko, and S. Podsiadlo, "Lattice parameters and anisotropic thermal expansion of hexagonal boron nitride in the $10-297.5 \text{ K}$ temperature range," vol. 75, no. 3, pp. 431-435, 2002.
- J. Wang, F. Ma, W. Liang, and M. Sun, "Electrical properties and applications of graphene, hexagonal boron nitride (h-BN), and graphene/h-BN heterostructures," vol. 2, pp. 6-34, 2017.
- A. Laturia, M. L. Van de Put, W. Vandenberghe, and Applications, "Dielectric properties of hexagonal boron nitride and transition metal dichalcogenides: from monolayer to bulk," vol. 2, no. 1, pp. 1-7, 2018.
- D. Wickramaratne, L. Weston, and C. Van de Walle, "Monolayer to bulk properties of hexagonal boron nitride," vol. 122, no. 44, pp. 25524-25529, 2018.
- H. O. Pierson, Handbook of refractory carbides and nitrides: properties, characteristics, processing and applications. William Andrew, 1996.
- N. Mittal, G. Kedawat, S. Gupta, and B. Kumar Gupta, "An Innovative Method for Large-Scale Synthesis of Hexagonal Boron Nitride Nanosheets by Liquid Phase Exfoliation," vol. 5, no. 40, pp. 12564-12569, 2020.
- K. A. Nekouee, R. Khosroshahi, R. T. Mousavian, and N. Ehsani, "Sintering behavior and microwave dielectric properties of $\text{SiO}_2\text{-MgO-Al}_2\text{O}_3\text{-TiO}_2$ ceramics," vol. 27, no. 4, pp. 3570-3575, 2016.
- H. Eslami-shahed and N. Ehsani, "The effects of adding CNTs and GNPs on the microstructure and mechanical properties of hexagonal-boron nitride," vol. 46, no. 14, pp. 22005-22014, 2020.
- J. P. Yasno and R. Kiminami, "Short time reaction synthesis of nano-hexagonal boron nitride," vol. 31, no. 10, pp. 4436-4443, 2020.
- B. Matsoso, W. Hao, Y. Li, V. Vuillet-a-Ciles, V. Garnier, P. Steyer, B. Toury, C. Marichy, C. Journet, "Synthesis of hexagonal boron nitride 2D layers using polymer derived ceramics route and derivatives," vol. 3, no. 3, p. 034002, 2020.
- F. Moravvej-Farshi, M. Amishi, and K. A. Nekouee, "Influence of different milling time on synthesized Ni-Zn ferrite properties by mechanical alloying method," vol. 31, no. 16, pp. 13610-13619, 2020.
- D. Li, C. Zhang, B. Li, F. Cao, S. Wang, K. Liu, Z. Fang, "Low-cost preparation of boron nitride ceramic powders," vol. 27, no. 3, pp. 534-537, 2012.
- A. Gomathi and C. Rao, "Nanostructures of the binary nitrides, BN, TiN, and NbN, prepared by the urea-route," vol. 41, no. 5, pp. 941-947, 2006.
- E. Budak, "Low temperature synthesis of hexagonal boron nitride by solid state reaction in the presence of lithium salts," vol. 44, no. 11, pp. 13161-13164, 2018.
- D. H. Besisa, M. A. Hagrass, E. M. Ewais, Y. M. Ahmed, Z. I. Zaki, and A. Ahmed, "Low temperature synthesis of nano-crystalline h-boron nitride from boric acid/urea precursors," vol. 17, no. 12, pp. 1219-1225, 2016.